Thermal Study of Accumulation of Conformational Disorders in the Self-Assembled Monolayers of C 8 and C 18 Alkanethiols on the Au(111) Surface

ARTICLE *in* LANGMUIR · APRIL 2005

Impact Factor: 4.46 · DOI: 10.1021/la048654z · Source: PubMed

7 AUTHORS, INCLUDING:

Prathima Nalam
University of Pennsylvania
17 PUBLICATIONS **135** CITATIONS
SEE PROFILE

Neeraj Rai
Mississippi State University
21 PUBLICATIONS **478** CITATIONS
SEE PROFILE

Chandrashekara Haramagatti
Asian Paints Research & Technology Centre
11 PUBLICATIONS **69** CITATIONS
SEE PROFILE

Ganapathy K Ayappa
Indian Institute of Science
96 PUBLICATIONS **1,777** CITATIONS
SEE PROFILE

Thermal Study of Accumulation of Conformational Disorders in the Self-Assembled Monolayers of C_8 and C_{18} Alkanethiols on the Au(111) Surface

N. Prathima,[†] M. Harini,[‡] Neeraj Rai,[‡] R. H. Chandrashekara,[§] K. G. Ayappa,[‡] S. Sampath,[§] and S. K. Biswas*,[†]

Departments of Mechanical Engineering, Chemical Engineering, and Inorganic and Physical Chemistry, Indian Institute of Science, Bangalore 560012, India

Received June 1, 2004. In Final Form: November 23, 2004

The thermal stability of short alkanethiol $CH_3(CH_2)_7SH$ (C_8) and long C_{18} self-assembled monolayers (SAMs) is investigated using grazing angle reflection−absorption infrared spectroscopy, cyclic voltammetry, and molecular dynamics simulation. We track the disordering of SAM by untilting and gauche defect accumulation with increasing temperature in the 300−440 K range, a range of interest to tribology. Molecular dynamics simulation with both fully covered and partially covered C_6, C_8, and C_{18} monolayers brings out the morphological changes in the SAM, which may be associated with the observed thermal stability characteristics. The molecular dynamics simulations reveal that short-chain C_6 and C_8 alkanethiols are more defective at lower temperature than the long-chain C_{18} alkanethiol. With increasing temperature disorder in the SAM, as reflected in both untilting and gauche defect accumulation, tends to saturate at temperatures below 360 K for short-chain SAMs such that any further increase in temperature, until desorption, does not lead to any significant change in conformational order. In contrast the disorder in the long-chain C_{18} SAM increases monotonically with temperature beyond 360 K. Thus, in a practical range of temperature, the ability of a SAM to retain order with increasing thermal perturbations is governed by the state of disorder prior to heat treatment. This deduction derived from molecular dynamics simulation helps to rationalize the significant difference we have observed experimentally between the thermal response of short- and long-chain thiol molecules.

Introduction

Self-assembled monolayers (SAMs) on various metallic surfaces have been used as models to study many phenomena such as wetting, adhesion, wear, friction, corrosion, and electron transfer across thin films.[1−8] One needs to understand the structure and stability of the monolayer to correlate the molecular properties of the SAMs to its physicochemical characteristics.[2] In tribology, generation of heat leading to temperature increases of the order of 373 K is not uncommon in lubricated contacts especially in the boundary lubrication regime. Knowledge of thermal stability of additive molecules, thus, leads us to better design and selection of these molecules for specific application. Here we focus on the effect of chain length on thermal stability with a view to understand why short-chain molecules may be preferred in tribological industrial practices.

Perhaps the most widely characterized SAMs are alkanethiols, $CH_3(CH_2)_{n-1}SH$ (C_n) on Au(111).[9−11] The chain length of the alkanethiol is an important parameter, which is known to have a significant effect on the structural properties of the monolayer. Longer-chain alkanethiols on gold are known to form ordered films because of increased van der Waals interactions between chains, and shorter-chain alkanethiols are generally more disordered.[12,13] The structure of long-chain alkanethiols self-assembled on gold has been studied extensively using vibrational spectroscopy [Fourier transform infrared (FT-IR) spectroscopy, and Raman spectroscopy],[12,14,15] X-ray diffraction (XRD),[16,17] electrochemistry,[18] and molecular dynamics (MD) simulations.[19,20] There is a general consensus, both in the experimental and in the molecular simulations literature, that there are two phase transitions, one at low temperatures between two ordered phases which differ in tilt directions and the other at high temperatures between an ordered phase and a disordered

* Corresponding author. Tel.: 091-080-22932351. Fax: 091-080-23600648. E-mail: skbis@mecheng.iisc.ernet.in.

† Department of Mechanical Engineering, Indian Institute of Science.

‡ Department of Chemical Engineering, Indian Institute of Science.

§ Department of Inorganic and Physical Chemistry, Indian Institute of Science.

(1) Kang, J. F.; Jordan, R.; Ulman, A. *Langmuir* **1998**, *14*, 3983.
(2) Whitesides, G. M.; Laibinis, P. E. *Langmuir* **1990**, *6*, 87.
(3) Jennings, G. K.; Munro, J. C.; Yong, T. H.; Laibinis, P. E. *Langmuir* **1998**, *14*, 6130.
(4) Laibinis, P. E.; Whitesides, G. M.; Allara, D. L.; Tao, Y. T.; Parikh, A. N.; Nuzzo, R. G. *J. Am. Chem. Soc.* **1991**, *113*, 7152.
(5) Mowery, M. D.; Kopta, S.; Ogletree, D. F.; Salmeron, M.; Evans, C. E. *Langmuir* **1999**, *15*, 5118.
(6) Zamborini, F. P.; Campbell, J. K.; Crooks, R. M. *Langmuir* **1998**, *14*, 640.
(7) Laibinis, P. E.; Whitesides, G. M. *J. Am. Chem. Soc.* **1992**, *114*, 9022.
(8) Yoshizawa, H.; Chen, Y.; Israelachvili, J. *Wear* **1993**, *168*, 161.
(9) Ulman, A. *Chem. Rev.* **1996**, *96*, 1533.
(10) Poirier, G. E. *Chem. Rev.* **1997**, *97*, 1117.
(11) Schreiber, F. *Prog. Surf. Sci.* **2000**, *65*, 151.
(12) Porter, M. D.; Bright, T. B.; Allara, D. L.; Chidsey, C E. D. *J. Am. Chem. Soc.* **1987**, *109*, 3559.
(13) Lio, A.; Charych, D. H.; Salmeron, M. *J. Phys. Chem. B* **1997**, *101*, 3800.
(14) Dubois, L. H.; Zegarski, B. R.; Nuzzo, R. G. *J. Chem. Phys.* **1993**, *98*, 678.
(15) Bryant, M. A.; Pemberton, J. E. *J. Am. Chem. Soc.* **1991**, *113*, 8284.
(16) Fenter, P.; Eisenberger, P.; Liang, K. S. *Phys. Rev. Lett.* **1993**, *70*, 2447.
(17) Fenter, P.; Eisenberger, P.; Burrows, P.; Forrest, S. R.; Liang, K. S. *Physica B* **1996**, *221*, 145.
(18) Widrig, C. A.; Chung, C.; Porter, M. D. *J. Electroanal. Chem.* **1991**, *310*, 335.
(19) Hautman, J.; Klein, M. L. *J. Chem. Phys.* **1989**, *91*, 4994.
(20) Hautman, J.; Bareman, J. P.; Mar, W.; Klein, M. L. *J. Chem. Soc., Faraday Trans.* **1991**, *87*, 2031.

10.1021/la048654z CCC: $30.25
Published on Web 02/15/2005

phase characterized by a larger number of gauche defects.[21] RAIRS (reflection−adsorption infrared spectroscopy)[22,23] thermal studies of long-chain alkanethiols on Au points to a gradual introduction of defects in the 300−350 K range where the decrease in the integrated peak intensity is attributed to the untilting of chains with very few gauche defects. Above 350 K the increase in peak intensity is attributed to increased disorder or melting of the monolayer.[23] This interpretation is consistent with MD simulations on long-chain alkanethiols.[21]

The electrochemical studies, on the other hand, show the above transitions to occur sharply in the 305−325 K range depending on the chain length.[24−26] The authors suggest that the transitions are irreversible and that the disordered state is a nonequilibrium state. In contrast to the RAIRS studies, electrochemical characterization is carried out in the presence of an electrolyte where both the application of an electric field across the metal/solution interface and ionic movement of the redox species toward the electrode are expected to influence the stability of the monolayer.

Short-chain alkanethiols, which are the focus of this manuscript, have not been subjected to the same scrutiny as their long-chain counterparts. Recent sum frequency generation spectroscopy[27] of short-chain SAMs ($n = 3-11$), which analyzes the orientation of the methyl groups, does not reveal a clear transition in behavior between short- and long-chain alkanethiols; however, a more gradual transition is observed as the chain lengths are decreased. Badia et al. have found the transition temperature to decrease gradually with decreasing chain length.[24] Fenter and co-workers, on the basis of the X-ray data, conclude that the C_{14} chain length divides the packing structure of alkanethiols assembled on gold into orthorhombic ($>C_{14}$) and monoclinic ($<C_{14}$).[17] There is also a general agreement that the thiols of chain length $<C_{14}$ are highly strained and disordered compared to the longer-chain versions of the same molecules.[12] The higher friction coefficients for short-chain SAMs obtained using friction force experiments[13,28,29] have been attributed to the greater disorder in short-chain SAMs when compared with the long-chain SAMs. Surface stress measurements[30] indicate that the stress increases linearly with chain length, with the smaller surface stress for the shorter chains being attributed to their inherent disorder. Although the transitions associated with changing the chain lengths have yet to be fully understood, it is clear that shorter-chain alkanethiols are generally more disordered than their longer-chain counterparts.

Understanding the role of defects and structure of domain formation during the preparation of the monolayer is common to both short- and long-chain SAMs and is an important aspect of the self-assembly process itself. The state of the monolayer depends, among other factors, on the immersion time of the Au substrate in the thiol solution and time−temperature history of the annealing procedure. Grazing incidence X-ray diffraction[16] illustrates that annealing increases the domain sizes from 10 to 100 nm for both short- and long-chain alkanethiols on Au. Scanning tunneling microscopy (STM) images on C_{12} indicate that as-deposited SAMs have line defects attributed to missing chemisorbed thiol molecules, resulting in straight-line or zigzag-shaped defects.[31] Larger domain sizes are formed as the monolayer is annealed. STM images of C_4 alkanethiols at room temperature[32] suggest the formation of ordered and disordered domains. The latter is being interpreted as a two-dimensional liquid. In the same study, liquidlike phases were not observed for C_8 and C_{10} alkanethiols.

Although the high-temperature behavior, which is the focus of this work, of long-chain alkanethiols has been studied using RAIRS, similar studies on short-chain alkanethiols are yet to appear in the literature. Because short-chain thiols are more defective at lower temperatures than the longer-chain counterpart, it is likely that the sequence of structural transitions that has been observed while heating the long chains will be different for the shorter-chain alkanethiols. In this manuscript we investigate the high-temperature thermal stability of C_8 and C_{18} alkanethiols on Au(111) using a combination of experimental and theoretical methods. Our sum of knowledge of the structural and entropic responses of thiols to thermal changes has two distinct experimental sources: (i) physical methods such as infrared spectroscopy or XRD being applied to dry SAMs and (ii) electrochemical methods where a SAM in a liquid experiences an electric field in an electrolyte environment. While the principle techniques used in the present work are infrared spectroscopy and MD simulation, we also carry out cyclic voltammetry in the 300−365 K range to delineate the dependence of our conclusions on the investigational technique. Constant-temperature MD simulations are used to obtain detailed information on structural properties such as tilt angles and gauche defects for C_6, C_8, and C_{18} SAMs. To study the influence of defects on the monolayer, MD simulations have been carried out for lower-coverage SAMs in the presence of line defects for initial configurations representative of a well-ordered monolayer and a highly defective monolayer. These simulations at lower coverages give us information on the thermal characteristics of domain growth and the effect of defects on the equilibrium properties of the system. Our theoretical and experimental studies indicate that there exists a large percentage of gauche defects in short-chain alkanethiols when compared to those in long-chain thiols, at a given temperature. The short-chain thiols being more defective untilt rapidly at lower temperatures when compared to long chains and, thus, are rendered structurally insensitive to further changes in temperature, in the temperature range of 300−390 K.

Experimental Section

Sample preparation methods for SAMs can have a profound influence on the results obtained. Hence, a highly reproducible substrate prepared using the vacuum evaporation technique of gold on glass surfaces is used in the present study. Gold films of 1500−2000 Å are deposited onto a clean glass surface that has been pre-covered with a 150-Å-thick chromium layer. Deposition

(21) Bhatia, R.; Garrison, B. J. *Langmuir* **1997**, *13*, 765.
(22) Bensebaa, F.; Ellis, T. H.; Badia, A.; Lennox, R. B. *J. Vac. Sci. Technol., A* **1995**, *13*, 1331.
(23) Bensebaa, F.; Ellis, T. H.; Badia, A.; Lennox, R. B. *Langmuir* **1998**, *14*, 2361.
(24) Badia, A.; Back, R.; Lennox, R. B. *Angew. Chem., Int. Ed. Engl.* **1994**, *33*, 2332.
(25) Gyepi-Garbrah, S. H.; Silerova, R. *Phys. Chem. Chem. Phys.* **2001**, *3*, 2117.
(26) Nakamura, T.; Aoki, K.; Chen, J. *Electrochim. Acta* **2002**, *47*, 2407.
(27) Nishi, N.; Hobara, D.; Yamanoto, M.; Kakiuchi, T. *J. Chem. Phys.* **2003**, *118*, 1904.
(28) Xiao, X.; Hu, J.; Charych, D. H.; Salmeron, M. *Langmuir* **1996**, *12*, 235.
(29) Brewer, N. J.; Beake, B. D.; Leggett, G. J. *Langmuir* **2001**, *17*, 1970.
(30) Berger, R.; Delamarche, E.; Lang, H. P.; Gerber, G.; Gemzewski, J. K.; Meyer, E.; Guntherodt, H. J. *Science* **1997**, *276*, 2021.
(31) Schonenberger, C.; Jorritsma, J.; Sondag- Huethorst, J. A. M.; Fokkink, L. G. J. *J. Phys. Chem.* **1995**, *99*, 3259.
(32) Poirier, G. E.; Tarlov, M. J.; Rushmeier, H. E. *Langmuir* **1994**, *10*, 3383.

is carried out at a rate of 1.0 Å/s for chromium and 4.0 Å/s for gold, and the substrate temperature is maintained at 573 K (300 °C) during the deposition, at a pressure of 2×10^{-5} mbar. The powder XRD data confirms the formation of a highly oriented ⟨111⟩ phase. The surface profiles taken using a profilometer (Taylor-Hobson, U.K.) give a reproducible average roughness of 12 ± 2 nm. The roughness factor calculated on the basis of the electrochemical redox reaction involving 0.5 M H_2SO_4 is 1.8.

The Au(111)/glass substrates are removed from the vacuum chamber of the coating unit and washed with methanol for 15 min before placing them into solution to ensure the removal of unwanted organic matter, which might have been deposited on the gold while transferring the gold slides from the coating unit to the desiccation chamber. Washing also removes fine glass particles that might spread onto the surface while cutting the gold slide. Between removal and washing, the substrates are transferred to a desiccator and kept under a vacuum of 5×10^{-2} mbar. The methanol used here is AR grade distilled methanol (Les Alcools De Commercial, Inc., Brampton, Ontario). The gold substrates are then immersed in a 3 mM solution of octadecanethiol or octanethiol (Aldrich, U.S.A.) in methanol at room temperature for a period of 24 h for octadecanethiol and 36 h for octanethiol. We performed experiments to calculate the optimum time of adsorption for C_8 and C_{18} thiol monolayers by monitoring the peak frequency of the antisymmetric CH_2 peak of the monolayers. The experiments were conducted with different adsorption times, 12−48 h. We find no change in the peak frequency value of d^- at room temperature for C_{18} and C_8 thiol SAMs for adsorption times greater than 24 and 36 h, respectively. After the adsorption, the substrates are removed from the solution, extensively rinsed using ethanol, and desiccated for drying. The samples are annealed for 1−2 h at room temperature in a vacuum (5×10^{-2} mbar) before making the IR and electrochemical measurements. The reproducibility of the formation of the SAM was assessed by the methylene (d^-) peak frequency. In the case of the C_{18} thiol we observed that SAM formation was highly reproducible; however, for the C_8 thiol a greater variability was observed.

IR Spectroscopy. All IR spectra reported here are taken using a Perkin-Elmer (Spectrum GX, Switzerland) FT-IR spectrometer equipped with a liquid nitrogen cooled mercury cadmium telluride detector. The variable temperature measurements for these monolayers are carried out in situ using a refractor reactor (Harrick, NY) accessory. The sample chamber and the heating accessory were purged using UHP (ultrahigh pure) nitrogen during initialization of the equipment for about 1/2 h. The system is not purged during the experiment. We used a fresh bare gold substrate for each new experiment. We clean the bare gold substrate with high-purity ethanol for 5 min, dry the sample in an UHP nitrogen jet, and desiccate it for 1/2 h before using it as a background in the IR experiment. The perpendicularly polarized infrared beam is reflected from the surface at an angle of 75° to the surface normal. All the spectra are averaged over 712 scans with a resolution of 4 cm^{-1} and referenced to the bare gold substrate. The spectral analysis is carried out using a spectrum 3.02 version (Perkin-Elmer) software. The temperature range used in the study is 303−440 K. The sample is heated uniformly and is allowed to equilibrate at each temperature for about 5 min before the spectrum is recorded.

Electrochemistry. The gold films are made into electrodes using conductive silver epoxy and copper leads. The contact point is effectively insulated before the adsorption is carried out. The electrodes are washed with ethanol and dried in a vacuum. The cleaning procedure is repeated until reversible cyclic voltammetric peaks are obtained with Fe^{2+}/Fe^{3+} (1 mM) solution. The electrodes are washed thoroughly with double-distilled water and kept in a vacuum to remove any trapped solvent molecules. These electrodes are then immersed in 3 mM thiol solution in methanol at room temperature for a period of about 24 h. After the SAM formation, the electrodes are cleaned with ethanol and kept in a desiccator before use.

Electrochemical experiments are carried out using a CH-660A electrochemical system (CH Instruments, U.S.A.). A conventional single-compartment, three-electrode cell is used with a calomel reference electrode and platinum foil counter electrode. The stability of the electrodes was checked, and after deposition of the SAM, the electrodes were heated and equilibrated until the current was found to be stable. This generally occurred after 8 min of equilibration, after which the voltammograms were obtained. Cyclic voltammetric experiments are performed in 1 mM deareated $Fe(CN)_6^{3-/4-}$ solution with 0.1 M KCl as the supporting electrolyte. The cyclic voltammograms are carried out in the potential range −0.2 to +0.6 V in the temperature range 300−365 K. The scan rate used is 50 mV/s. In electrochemistry a single sample was used for the exploration of the entire temperature range from 300 to 365 K, and this procedure was repeated with five different samples. The samples survive multiple cycles in the $Fe(CN)_6^{3-/4-}$ solution at room temperature. We see no change in the cyclic voltammograms after conducting a few repeated cycles.

MD Simulations. Constant-temperature MD simulations have been carried out using a Nose-Hoover thermostat.[33] The interatomic potential parameters were identical to those used in an earlier united atom MD simulation of alkanethiols assembled on a structureless gold surface.[19] In the united atom model the CH_2 and CH_3 groups in the alkane chain are treated as spherical atoms. The intramolecular force field consists of torsional potentials, bending potentials, and Lennard-Jones (LJ) interactions between every fourth united atom within the chain. Intermolecular interactions were treated using a 12−6 LJ potential. The Au−S−C bond is assumed to be flexible, and the interaction between the thiol molecule and the gold surface is a one-dimensional interaction potential, which depends only on the normal distance of the atoms from the surface. There has been considerable debate in the literature[19,34,35] on the most suitable model to mimic the thiol−gold interaction. While the assumptions related to the smoothness of the gold substrate and the flexibility of the Au−S−C bond have been found to make some difference in the prediction of gauche defects, tilt angles, and film thickness, the differences are generally small. As our primary interest here is to compare the effect of chain length on the structural properties of SAMs, we have chosen to use a flexible Au−S−C bond anchored to a flat, rigid gold surface. The results from the constant-temperature NVT simulation for C_{16} were in excellent agreement with those reported in the literature.[36] As an additional check we also found similar results from a microcanonical ensemble (NVE) simulation with results obtained from the NVT simulation. The time step used for the MD simulations was 4 fs, and run lengths were 320 ps for C_6 and 480 ps for C_8 and C_{18} with half the time used for equilibration. To check if these run lengths were adequate, longer simulation run lengths were carried out for a few cases and the results were found to be unaltered. In the case of C_8 at 360 K the changes between equilibration run lengths consisting of 320 and 480 ps revealed that the uncertainty in the system tilt, percentage of gauche defects, and total energies were 0.03°, 0.3%, and 0.054 kJ/mol, respectively.

NVT simulations have been carried out for C_6, C_8, and C_{18} alkanethiols. In the case of the fully covered (FC) SAMs, 360 thiol molecules were used on a periodic box of length $L_x = 89.48$ Å and $L_y = 86.10$ Å. This yields a surface density $\rho_s = 21.4$ Å^2/chain for a face-centered cubic arrangement of sulfur atoms containing three atoms per unit cell with a lattice parameter of 4.97 Å. Simulations have also been carried out at surface densities that are lower than $\rho_s = 21.4$ Å^2/chain. For the lower densities, 333 molecules were used which correspond to a coverage of 92.5% and a surface density of $\rho_s = 19.795$ Å^2/chain. In the case of the low-coverage (LC) SAMs two different initial configurations were investigated. In the first case a FC monolayer was prepared with the chains in a herringbone arrangement having an all-trans conformation. The lower coverage (density) was achieved by removing thiol molecules creating line defects as illustrated in Figure 1. Two types of LC situations were investigated which differ only in the initial state of the monolayer. In the first case, henceforth referred to as LC1, the chains were in an all-trans conformation. In the second case, henceforth referred to as LC2,

(33) Nose, S. *Mol. Phys.* **1984**, *52*, 255; *J. Phys. Chem.* **1984**, *81*, 511.
(34) Rai, B.; Sathish, P.; Malhotra, C. P.; Pradip; Ayappa, K. G. *Langmuir* **2004**, *20*, 3138.
(35) Rong H.; Frey, S.; Yang, Y.; Zharnikov, M.; Buck, M.; Wuhm, M.; Woll, C.; Helmchen, G. **2001**, *17*, 1582.
(36) Hautman, J.; Klein, M. L. *J. Chem. Phys.* **1990**, *93*, 7483.

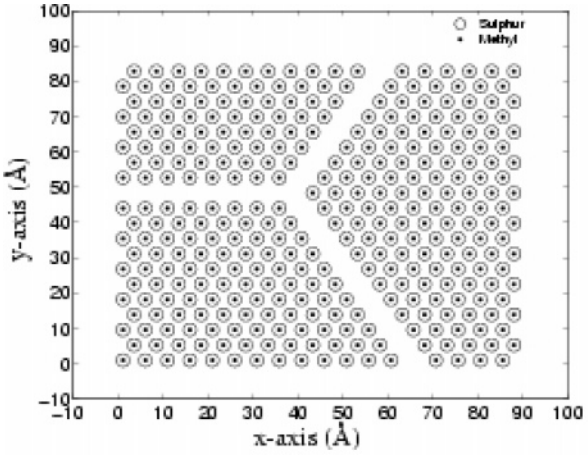

Figure 1. Top view of the initial configuration of the LC all-trans SAM (LC1) used in the MD simulations.

the initial arrangement was prepared from a monolayer that was equilibrated at 400 K in the case of the C_8 and C_{18} SAMs and to 300 K in the case of the C_6 SAM. The initial configuration used for LC2 corresponds to a highly defective monolayer with a large percentage of gauche defects. The initial configurations of LC1 and LC2 correspond to monolayers with the same surface density with similar line defect topologies.

Results

Infrared Spectroscopy. Figure 2 shows representative spectra for both C_8 and C_{18} thiol SAMs on the Au(111) surface at three different temperatures. The peaks are indexed for different modes as given in Table 1. We use the peak frequency levels of the methylene stretches (and not the methyl stretches) as a yardstick for order in the SAM because the terminal methyl groups could be prone to water adsorption in ambient experiments. At 303 K the position of the antisymmetric methylene stretch (d^-) at 2918 cm^{-1} reveals that the long-chain SAM is well ordered when compared with the peak for the short-chain thiol at 2921 cm^{-1}. The peak frequencies, integrated intensities, and line widths have been recorded continuously in the 303−440 K range of temperature. The methylene scissors deformation mode at 1459 cm^{-1} and symmetric methyl deformation mode at 1364 cm^{-1} are also observed (not shown). However, the signals for these modes are weak, and although they do show temperature dependence of peak frequencies and integrated intensities, these results are not discussed here because they do not provide any additional information to what we infer from the main range of the frequency (2800−3000 cm^{-1}).

Figure 3 shows the variation of the peak frequency for the antisymmetric methylene stretch (d^-) for both the thiol molecules as a function of temperature. The peak frequency in C_8 does not change significantly in the 300−380 K range while for the same temperature range C_{18} increases almost monotonically. We see a sharp rise in the peak frequency for the C_8 thiol at temperatures higher than 390 K (Figure 3). Also at these higher temperatures the uncertainty in the C_{18} peak frequency as reflected in the larger error bars increases. This increase in frequency for both the thiols could be attributed to desorption. Figure 4a,b shows the integrated intensity shift of the antisymmetric methylene stretch (d^-) of the C_8 thiol and the C_{18} thiol, respectively. The integrated intensity for C_8 is in marked contrast to the data for C_{18}. In the temperature range 300−360 K the intensity decreases by 2×10^{-4} au/K, in the 360−392 K range, the decrease slows down by about half (1×10^{-4} au/K) of that in the previous range, and at a temperature of about 392 K there is a sharp

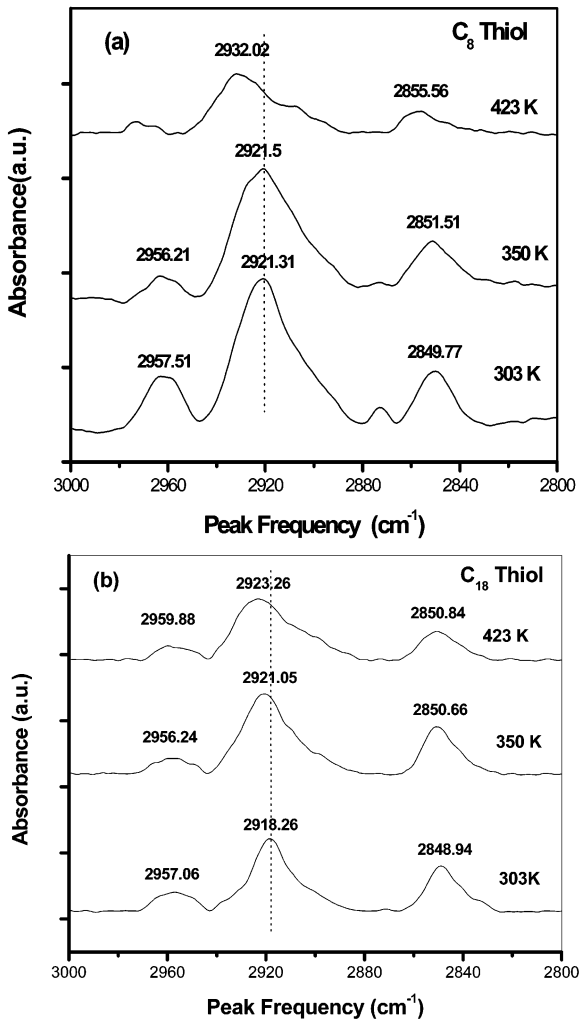

Figure 2. FT-IR spectra of the (a) C_8 and (b) C_{18} alkanethiols at 303, 350, and 423 K.

Table 1. Infrared Vibrational Stretching Frequencies of CH_2 and CH_3 Modes for the C_8 and C_{18} Alkanethiols on Au(111) at 303 K

	C_8 thiol		C_{18} thiol	
assignment[a]	observed	reported (C_8)[b]	observed	reported (C_{18})[b]
CH_2, d^-	2921	2921	2918	2917
CH_2, d^+	2850	2851	2849	2850
CH_3, r^-	2962	2966	2965	2965
CH_3, r^+	2872	2878	2878	2879

[a] d^-, d^+, r^-, and r^+ correspond to methylene antisymmetric, methylene symmetric, methyl antisymmetric, and methyl symmetric stretches, respectively, at room temperature. [b] Reference 12.

decrease in intensity (Figure 4a). The monotonic changes we observe in the integrated intensity for C_8 are in contrast to what has been reported in a previous IR study on a long-chain molecule where a decrease in intensity in the lower (<350 K) temperature range is attributed to a single cause, untilting.[23] This is followed by an increase in intensity in the higher (>350K) temperature range, attributed to gauche defect accumulation. Both of these contribute to an increase in SAM disorder as reflected in an increase in peak frequency.[23] Although we did not observe this trend in some of the repeated experiments (Figure 4b), the difference between the present and the literature data may be attributed to the difference in the

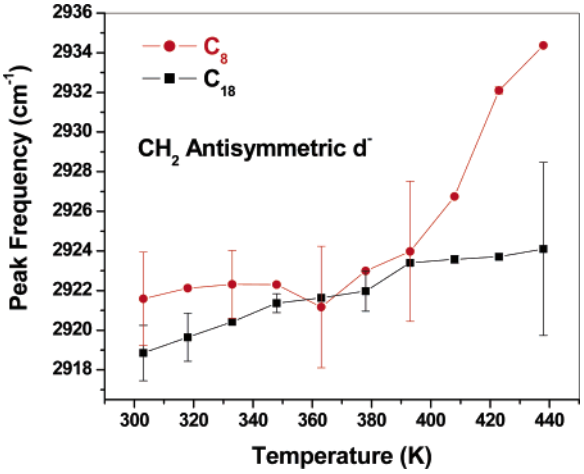

Figure 3. Temperature dependence of the peak frequency of the methylene antisymmetric stretch (d^-) from IR for the C_8 and C_{18} alkanethiols. The higher peak frequency values for the C_8 thiol reflect greater disorder when compared with those of the C_{18} SAM.

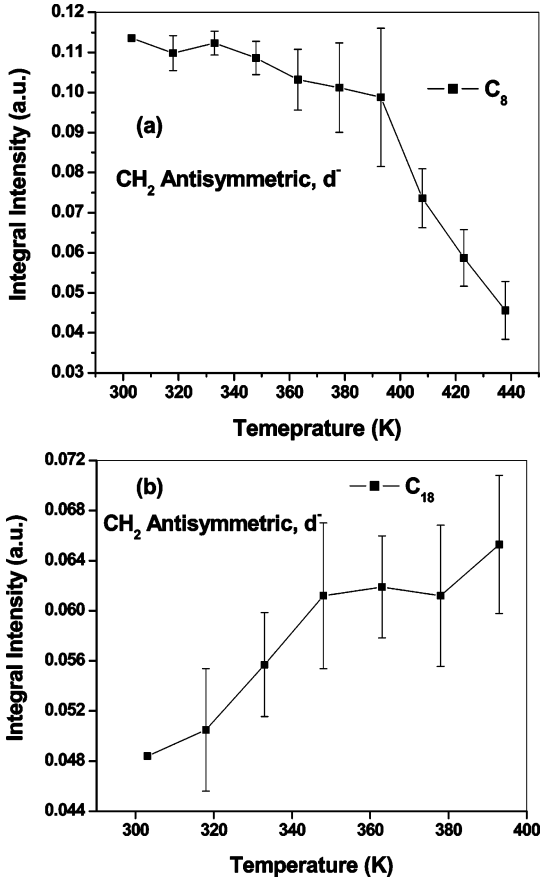

Figure 4. Temperature dependence of the integrated intensity of the methylene antisymmetric stretch (d^-) from IR for the (a) C_8 and (b) C_{18} alkanethiols. In contrast to that of the C_{18} SAM, the integral intensity for the C_8 SAM monotonically decreases with increasing temperature.

thermal histories in the samples. We see a decrease in the integrated intensity for the C_{18} thiol after 400 K (not shown), which can be attributed to desorption as referred by Ellis et al.[23] Figure 5a,b shows the intensity of methylene d^+ stretch and the methyl r^+ stretch for the C_8 thiol, respectively. The weak methylene d^+ stretch peak shows a trend similar to that observed for the d^- peak intensity (Figure 4a).

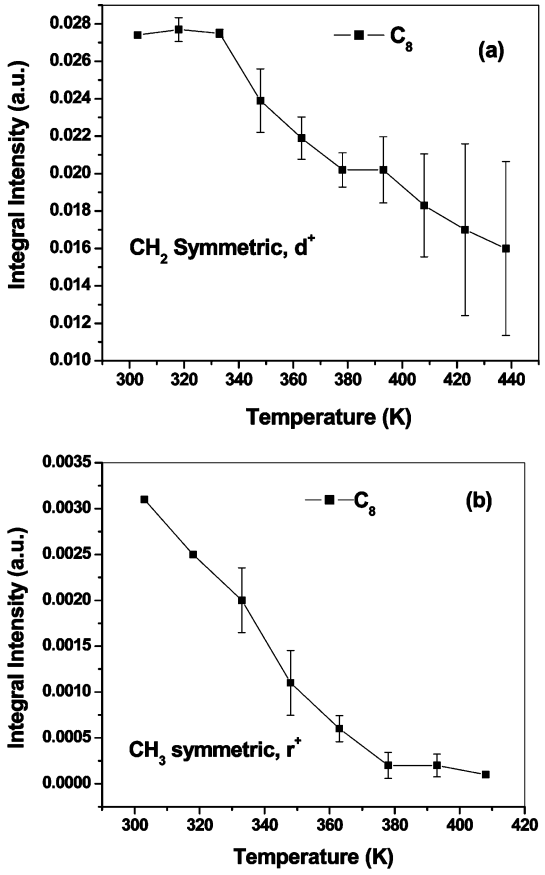

Figure 5. Temperature dependence of the integrated intensity shift from IR for the (a) methylene symmetric stretch (d^+) and (b) methyl symmetric stretch (r^+) of the C_8 alkanethiol.

Cyclic Voltammetry. The temperature dependence of the Fe^{3+} reduction current averaged from five different experiments in the 300−365 K range for the C_8 and C_{18} thiols is shown in Figure 6a,b, respectively. In the 300−330 K temperature range the observed currents are more or less the same for both the C_8 and the C_{18} thiol based monolayers. In this temperature range the currents are also insensitive to thermal changes. At about 330 K the currents for both the thiols start to increase sharply indicating perhaps an order-to-disorder phase transition. The current for the C_{18} thiol increases from 1.5 to 25 $\mu A/cm^2$ in the 330−360 K range, indicating a continuous increase in molecular disorder with increasing temperature. The increase in current for the C_8 thiol in the same temperature range is from 1.5 to 9 $\mu A/cm^2$, suggesting that shortening the molecules arrest, to some extent, the rate at which molecular disorder increases with temperature. The currents recorded in these experiments reflect the blockage or otherwise of the ionic movement of the redox species toward the electrode surface. This accessibility may be related to molecular order, domain structure, and monolayer thickness. The high-temperature data of ionic blockage, however, does bring out the fact that the C_{18} SAM becomes increasingly penetrable with temperature, while the response of the C_8 SAM indicates a somewhat greater thermal stability than that observed for the C_{18} SAM. This is also the conclusion that we have reached in this paper from IR study of dry SAMs and MD simulation. This is an important conclusion because the temperature range is of practical interest to tribology.

MD Simulations. Figure 7 illustrates the system tilt as a function of temperature for FC, LC1, and LC2 SAMs for C_6, C_8, and C_{18} thiols, and the corresponding gauche

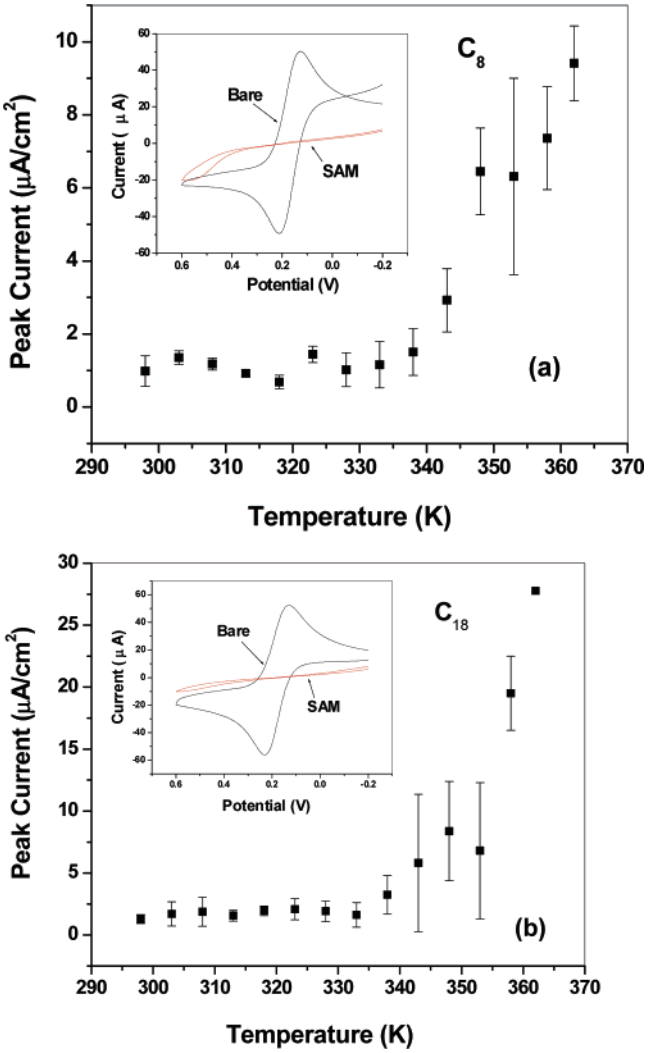

Figure 6. Temperature dependence of the Fe^{3+} reduction current for (a) C_8 and (b) C_{18} alkanethiols obtained from cyclic voltammetry experiments. Insets illustrate the voltammograms with and without (bare electrode) the SAM at $T = 298$ K. For both C_8 and C_{18} the peak currents are relatively insensitive to temperature below 330 K.

defect percentages are illustrated in Figure 8. The system tilt was computed by averaging the tilt angle obtained for the individual chains in the SAM. The tilt angle for a single chain is defined as the angle found between the line joining the sulfur atom to the CH_3 group and the normal to the substrate. A gauche defect was assumed to occur when the dihedral angle $\phi < -60°$ and $\phi > 60°$. The values reported are based on averages computed for all the dihedral angles in the monolayer. We note that the MD simulations are carried out for temperatures in the 100−450 K range. For both the short- and long-chain thiols, LC monolayers have higher tilt angles when compared with the FC monolayer. This increase in tilt angle with decreasing surface density has also been observed in a MD study by Bareman and Klein.[37] Although the LC SAMs have a higher percentage of gauche defects, the availability of a greater free volume in the case of the LC SAMs leads to a higher tilt angle. The decrease in tilt angles with increasing temperature for the FC and LC monolayers is accompanied by an increase in the gauche defects as seen in Figure 8. This trend is observed for both long and short chains. The deviation from this trend occurs

(37) Bareman, J. P.; Klein, M. L. *J. Phys. Chem.* **1990**, *94*, 5202.

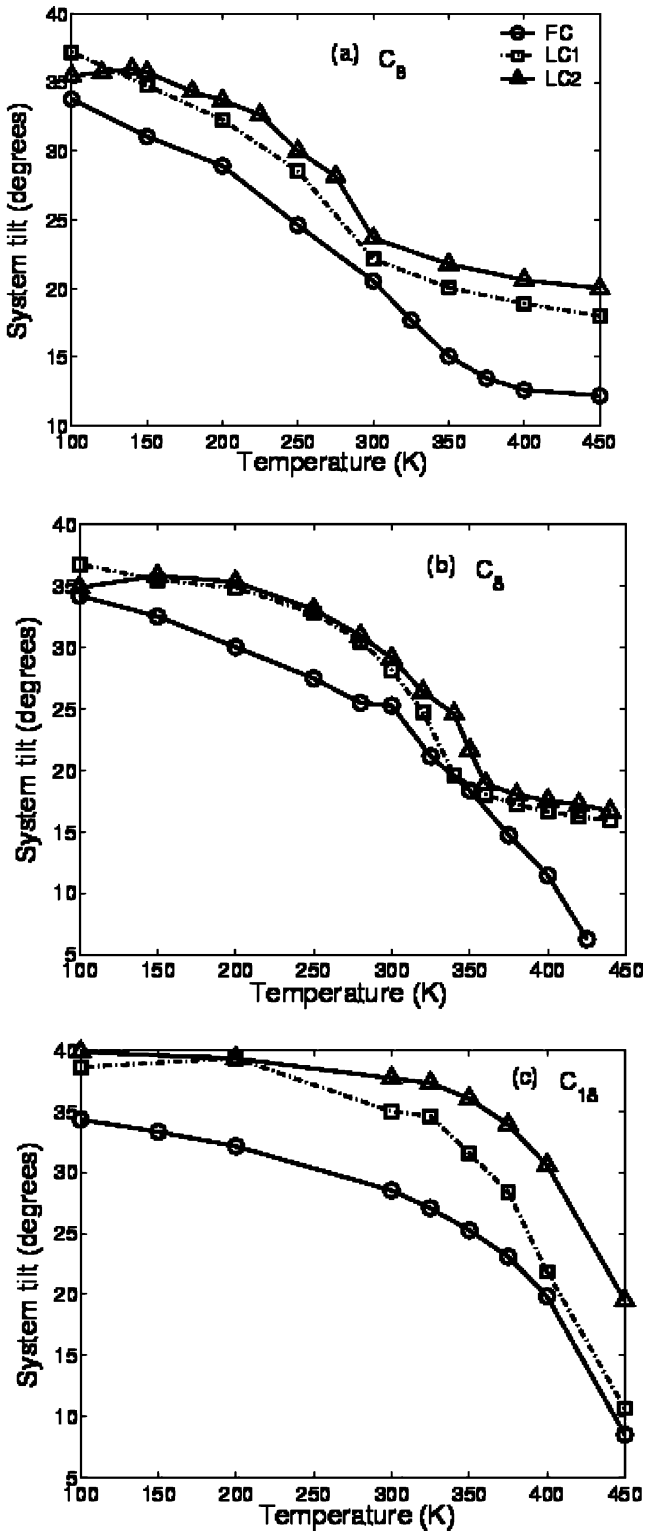

Figure 7. Temperature dependence of the system tilt for FC, LC1, and LC2 SAMs for the (a) C_6, (b) C_8, and (c) C_{18} alkanethiols obtained from MD simulation. The monotonic decrease in the system tilt observed for C_{18} SAMs is not observed in the cases of C_6 and C_8 SAMs. The tilt angle for the LC SAMs is always greater than that of the FC SAMs.

for C_6 and C_8 at lower temperatures $100 < T < 150$ K (Figure 7a,b), where a small increase in tilt angle is observed. In the same temperature range, gauche defects are seen to decrease (Figure 8a,b). This improved ordering of the film is akin to the process of thermal annealing used to remove defects in as-deposited SAMs. The MD

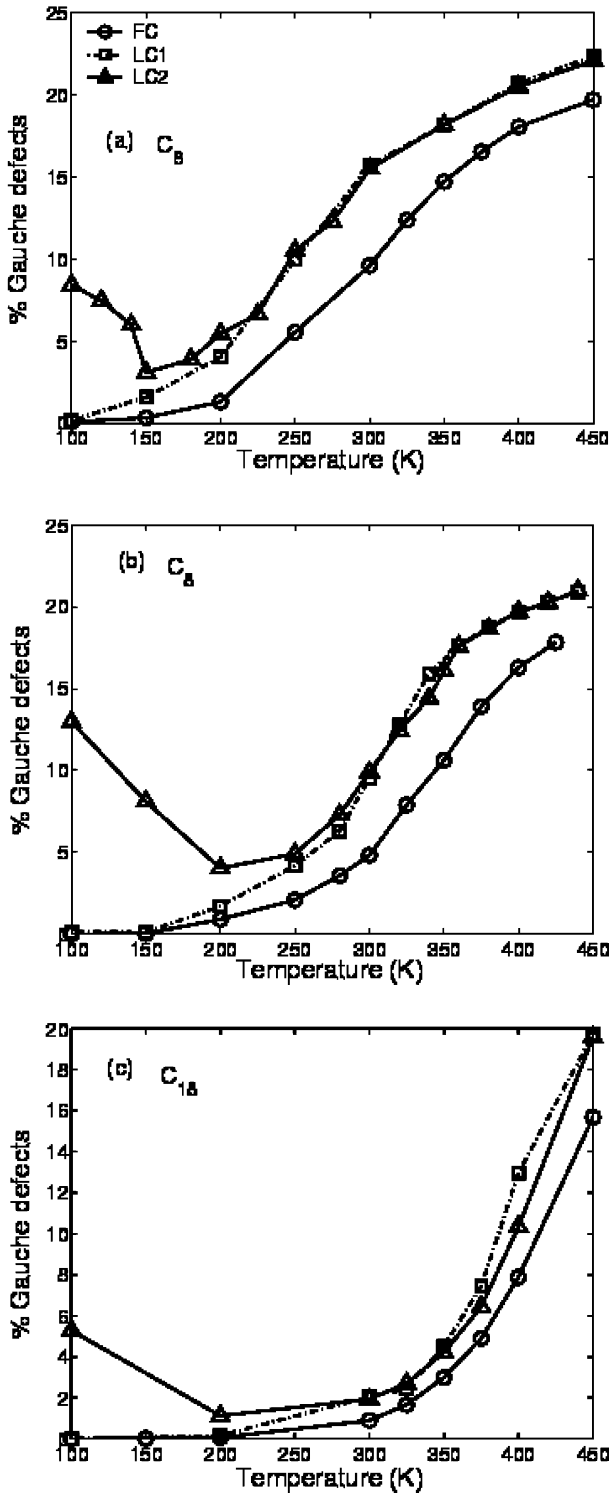

Figure 8. Temperature dependence of the gauche defects for FC, LC1, and LC2 SAMs for the (a) C_6, (b) C_8, and (c) C_{18} alkanethiols obtained from MD simulation. Similar to the trends observed in the system tilt (Figure 7) the gauche defect percentage increases monotonically with temperature for the C_{18} SAMs and saturates at lower temperatures for C_6 and C_8 SAMs.

simulation, thus, indicates that it is possible to anneal defective SAMs. Clearly the annealing temperature depends on the initial state of disorder; for the level of disorder in the LC2 SAM at 100 K, the annealing temperature as reflected in the gauche defects for both C_8 and C_{18} SAMs is around 250 K.

In contrast to C_{18}, the shorter chains (C_6 and C_8) are significantly more disordered and the gauche defect percentage (Figure 8) for LC1 SAMs at 300 K increases to 2% for C_{18} and 10 and 16% for C_8 and C_6, respectively. The corresponding tilt angles (Figure 7) at 300 K are 35, 28, and 22° for the C_{18}, C_8, and C_6 LC1 SAMs, respectively. Increasing the temperature above 300 K, the C_8 LC SAM untilts rapidly by 10° and the gauche defects multiply from 10 to 17%, in the 300−360 K range (Figures 7b and 8b), respectively. In this temperature range the gauche defect percentage for the initially (300 K) less defective C_{18} LC SAM more than doubles (from 2 to 5%), while there is a modest decrease of 4° in the system tilt. The untilting and gauche defect accumulation for the highly defective C_8 SAM (17% gauche defect) at temperatures above 360 K is arrested while the (5% gauche defective) C_{18} SAM continues to untilt and accumulate defects steadily in the 360−450 K range. This temperature at which the untilting and defect accumulation saturates is less than 300 K for C_6 and 360 K for C_8. We refer to this temperature as the saturation temperature (T_s) that increases with chain length. It has to be noted here that while the structural change is retarded greatly at T_s, the molecules continue to untilt (C_8 untilts by 2.1° in the 360−450 K range) and accumulate defects (gauche defect goes up for C_8 from 17 to 21% in the 360−450 K range) albeit very slowly at temperatures above T_s.

Although the above discussion is based on the results for the LC SAMs, similar trends are observed for the FC SAMs. Further, because the as-deposited SAMs in experiments are defective the results for LC SAMs would be more indicative of the actual experiments. The character of this transition to saturation is revealed succinctly in the snapshots of molecular conformations obtained from the MD simulation. Figures 9 and 10 show the snapshots of the $x-y$ projection of the C_8 and C_{18} LC SAMs, where one end of each individual line segment represents the position of the sulfur while the other end represents the methyl group. For a given molecule the length of the segment is an indicator of the tilt. The shorter the segment, greater is the molecule untilt. Figure 9 reflects the trends set out in Figures 7 and 8. At 300 K the snapshots (Figure 9a) for the LC SAMs of the C_8 thiol reveal that the molecules in the monolayer are uniform with regard to both the tilt direction and the tilt angle (28°). The snapshot for the C_8 SAM at 340 K (Figure 9b) shows a highly defective monolayer with great variation in the tilt angles and no preferred tilt direction. On closer examination we note that the defects consist of pinwheel structures where an untilted molecule is surrounded by other molecules with large tilt angles. Interestingly these pinwheel structures have been observed at the onset of disorder in molecular simulation studies of the adsorption of N_2 on graphite.[38] The snapshots at 360 and 440 K (Figure 9c,d) reveal films that are highly defective with no apparent difference in disorder between them, as reflected in the randomness in tilt and molecular orientation. In such a configuration there is a lack of long-range order, and the SAM may be regarded as almost amorphous.

Increasing the temperature of a partially covered SAM allows easy untilting and defect accumulation to utilize the vacant spaces until the defect population saturates. We have observed the randomization of the molecules initiated by the formation of the pinwheel structure even at 330 K (Figure 9b shows it at 340 K). Thus, we may state that for the short-chain C_8 alkanethiol gauche defects increase and the tilt angles start to decrease at about 320

(38) Kamakshi, J.; Ayappa, K. G. *Langmuir* **2001**, *17*, 5245.

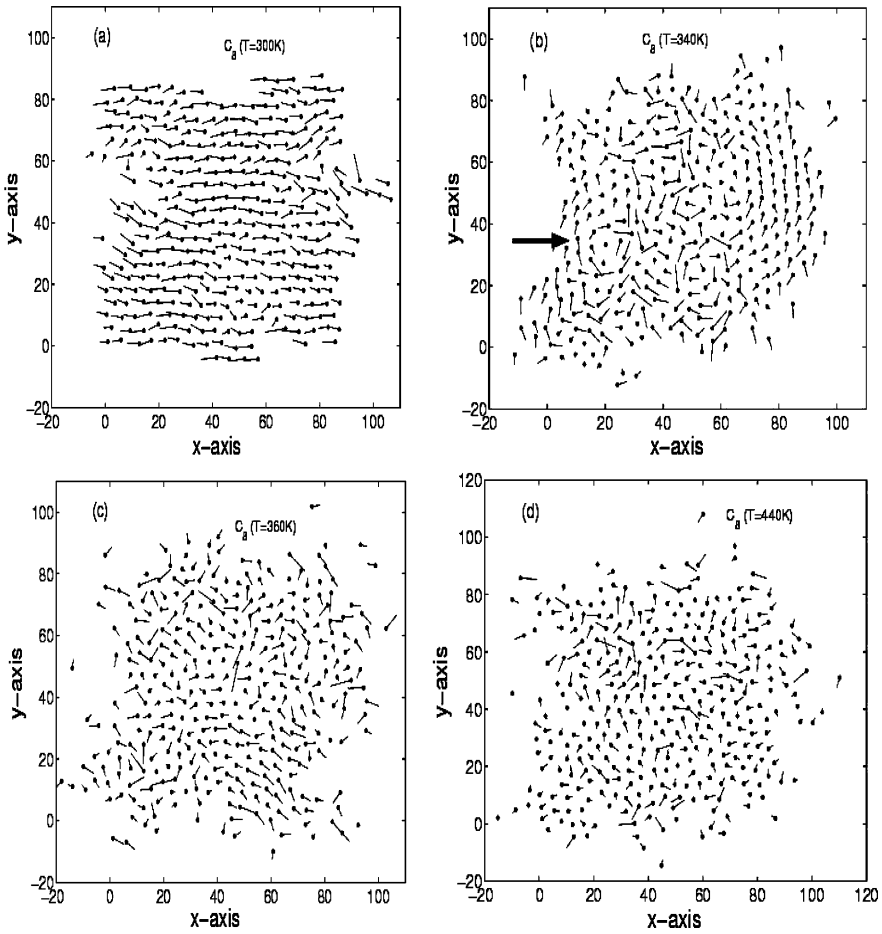

Figure 9. Snapshots of the $x-y$ projection for the C_8 alkanethiol from MD simulation at (a) 300, (b) 340, (c) 360, and (d) 440 K. The arrow illustrates the pinwheel defect, and the axis units are in angstroms. The line segments are obtained by joining the sulfur atom to the terminal methyl group. At temperatures above 340 K, the monolayer does not possess a uniform tilt direction as observed at 300 K.

K (Figures 7 and 8), and aided by rapid untilting and defect accumulation in this state, it completes the saturation process by 360 K. Increasing the temperature above 360 K appears to keep the gauche defect population and the molecules nearly saturated. The high levels of energy associated with the system at higher temperatures may be adequate for desorption of the molecule.

For the much less defective C_{18} molecule, untilting and defect accumulation continue to temperatures well above 400 K as shown in Figures 7 and 8. This is reflected in the snapshots (Figure 10a−d) which reveal that the SAM is able to retain its uniformity in the tilt direction until around 400 K (Figure 10b). The pinwheel structures associated with the onset of disorder starts to appear (Figure 10c) in the snapshots from about 425 K. At 450 K we see a randomized configuration (Figure 10d), giving a value of T_s between 425 (Figure 10c) and 450 K, which is significantly higher than that for C_8. Higher temperatures are, therefore, needed for longer-chain molecules to accumulate the same saturation level of defects, when compared with shorter chains.

It is interesting to examine the influence of defects on contributions to the internal energy of the monolayer. The total potential energy as shown in Figure 11 reveals that the LC2 SAMs have the highest energies at lower temperatures as the configurations correspond to molecules with a large number of gauche defects. As the temperature is increased the potential energies of both the LC1 and the LC2 SAMs are nearly identical, indicating that these SAMs are energetically equivalent at higher temperatures. The temperature at which this equivalence in energies is observed between the LC SAMs increases with increasing chain length. These temperatures can be approximately identified as 200, 225, and 300 K for the C_6, C_8, and C_{18} SAMs, respectively. We point out that the departure in the trends in potential energies for the LC2 SAMs at lower temperatures is primarily due to the differences in the initial configuration, leading to a film that is in a metastable state, and, hence, the energetics are likely to be influenced by the length of the MD simulations. However, longer simulations up to 640 ps did not alter the results for both the short- and the long-chain LC2 SAMs. The saturation temperatures, which were defined to indicate the temperature above which structural changes are rapidly retarded, are also reflected in the internal energies. The differential change in the total potential energy of the monolayer with increasing temperature reflects transitions at 300 and 360 K for C_6 and C_8 LC monolayers (Figure 11a,b). Although the saturation effect is less pronounced for the FC SAMs the potential energies level out at higher temperatures for both C_6 and C_8 alkanethiols. In contrast the total potential energy for the C_{18} monolayer continuously decreases (becomes more positive) with increase in temperature (Figure 11c). Similar trends are reflected in the intramolecular potential energies that increase (more negative) with temperature.

Although the energetic contributions (not shown) from torsional, intermolecular, and Au substrate interaction all reveal that the LC2 SAMs are the least favored

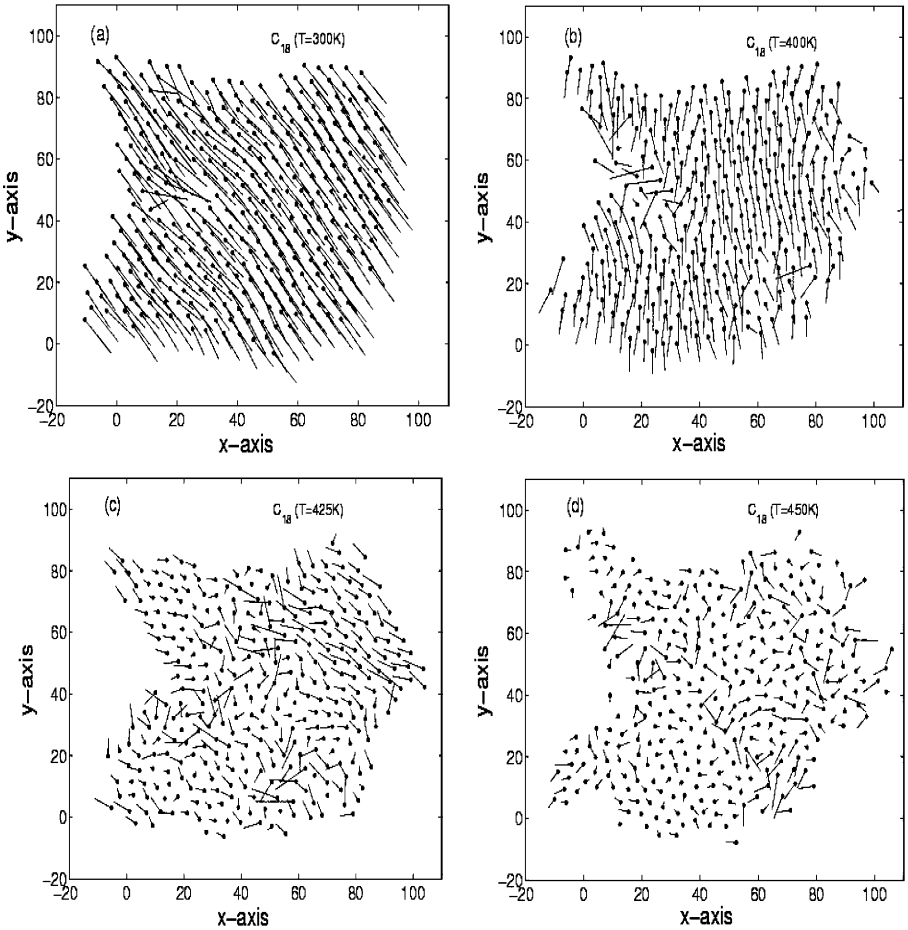

Figure 10. Snapshots of the $x-y$ projection for the C_{18} alkanethiol from MD simulation at (a) 300, (b) 400, (c) 425, and (d) 450 K; the axis units are in angstroms. In contrast to that of the C_8 thiol (Figure 9), the C_{18} alkanethiol monolayer possess a uniform tilt direction up to 400 K.

energetically, the intramolecular potentials (Figure 12) show an opposite trend. Introduction of defects increases the van der Waals interaction within the chain at low temperature, and this is reflected in the favorable intramolecular interactions for the LC SAMs when compared with those for the FC SAMs. However, the energetic benefit from the intramolecular interaction is less than 0.5 kJ/mol and, hence, has little influence on the overall energetics of the film.

Interpretation of IR Results. In attempting to interpret the difference in trends observed in the integrated intensity of the IR results we point out that the MD results are obtained using an all-atom model. Because the integrated intensity of the CH_2 vibrational modes reflects the population of IR active modes that couple with the electric field, MD is expected to provide only a qualitative explanation of the trends in the IR data.

The MD simulation clearly indicates that the gauche defect accumulation and untilt always accompany each other though to a greater or a lesser extent in different regimes of temperature. As a result, the IR integrated intensity data are always a resultant of two opposing trends with increasing temperature: an increase in intensity and a reduction in intensity, due to an increase in gauche defects and an increase in untilt, respectively.[23] The MD simulations for the C_{18} LC SAM, in the 300−360 K temperature range, show that the gauche defects accumulate fast (2.5 times) and untilt happens slowly (3.5°) with increasing temperature (Figure 8c). The resultant increase in integrated intensity seen for C_{18} may, thus, reflect a SAM becoming disordered primarily because of gauche defect accumulation (Figure 4b). At temperatures higher than 360 K the untilting and gauche defect accumulation (Figures 7c and 8c) occur simultaneously and the increase in integrated intensity slows down considerably (Figure 4b), reflecting a strong role of untilting in the disordering process at these higher temperatures. For C_8 thiols the MD simulation shows the gauche defects to increase 1.8 times in the 300−360 K regime while the molecules untilt by 10° indicating a dominance of the untilt phenomenon in the disordering process. The reduction in integrated intensity seen in Figure 4a in the 300−360 K regime must, therefore, be largely influenced by untilt.

One of the main contributions of our MD study is to point out that, when a SAM is highly prone to defect accumulation at lower temperatures (short-chain C_8 thiol) the defects accumulate quickly with increasing temperature and start to saturate at a relatively modest temperature of 320 K where the SAM begins to acquire a randomized morphology. Such a state, which becomes frozen by about 360 K, arrests further accumulation of defects and molecular mobility and continues to a high temperature, 390 K, where there is a sudden increase in mobility, which perhaps leads to desorption. We tested this by thermally cycling the C_8 thiol SAM and found that the room-temperature peak frequency can be recovered on cooling as long as the heat treatment temperature is less than 390 K. When the peak temperature of the thermal cycle is greater than 390 K, there is always a residual disorder on cooling back to room temperature, even when the cooled SAM has been aged at room temperature for

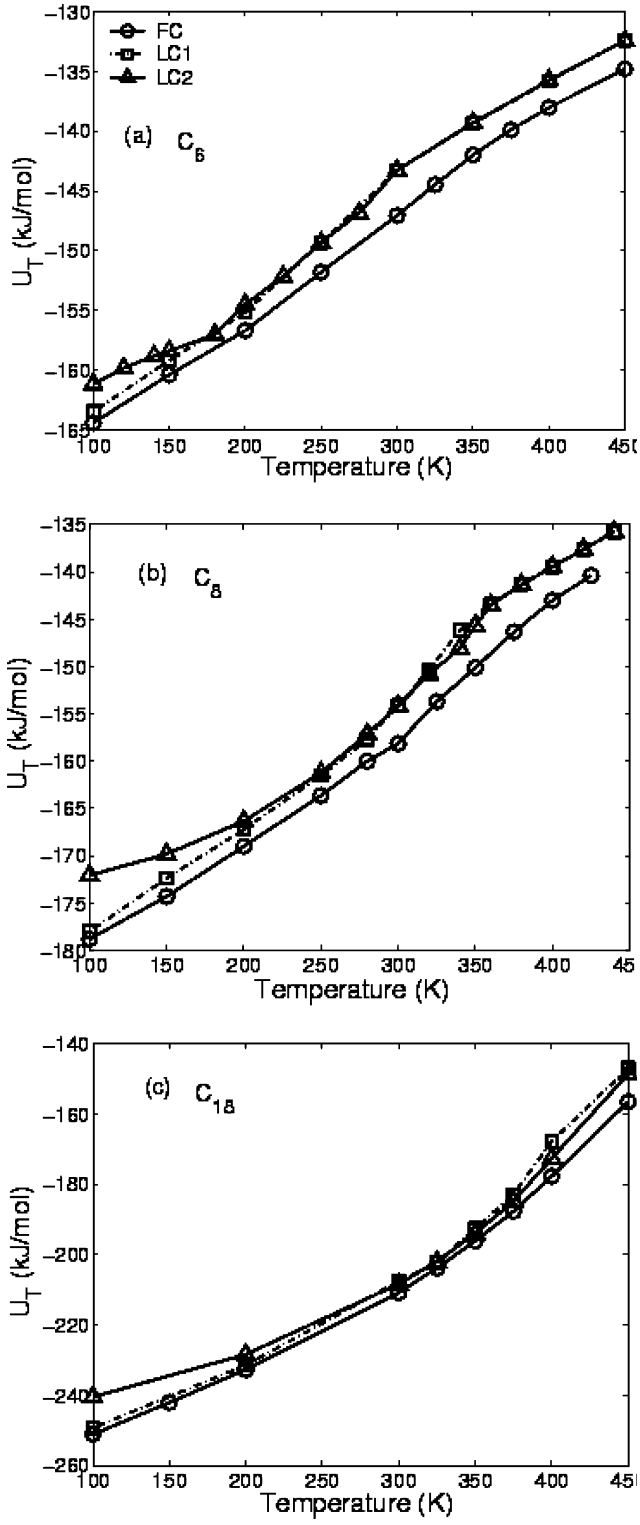

Figure 11. Temperature dependence of the total potential energy (U_T) for FC, LC1, and LC2 SAMs for the (a) C_6, (b) C_8, and (c) C_{18} alkanethiols from MD simulation. U_T for the FC SAMs is always lower than that for the LC SAMs. At higher temperatures, the U_T values for both the LC1 and the LC2 SAMs are nearly identical.

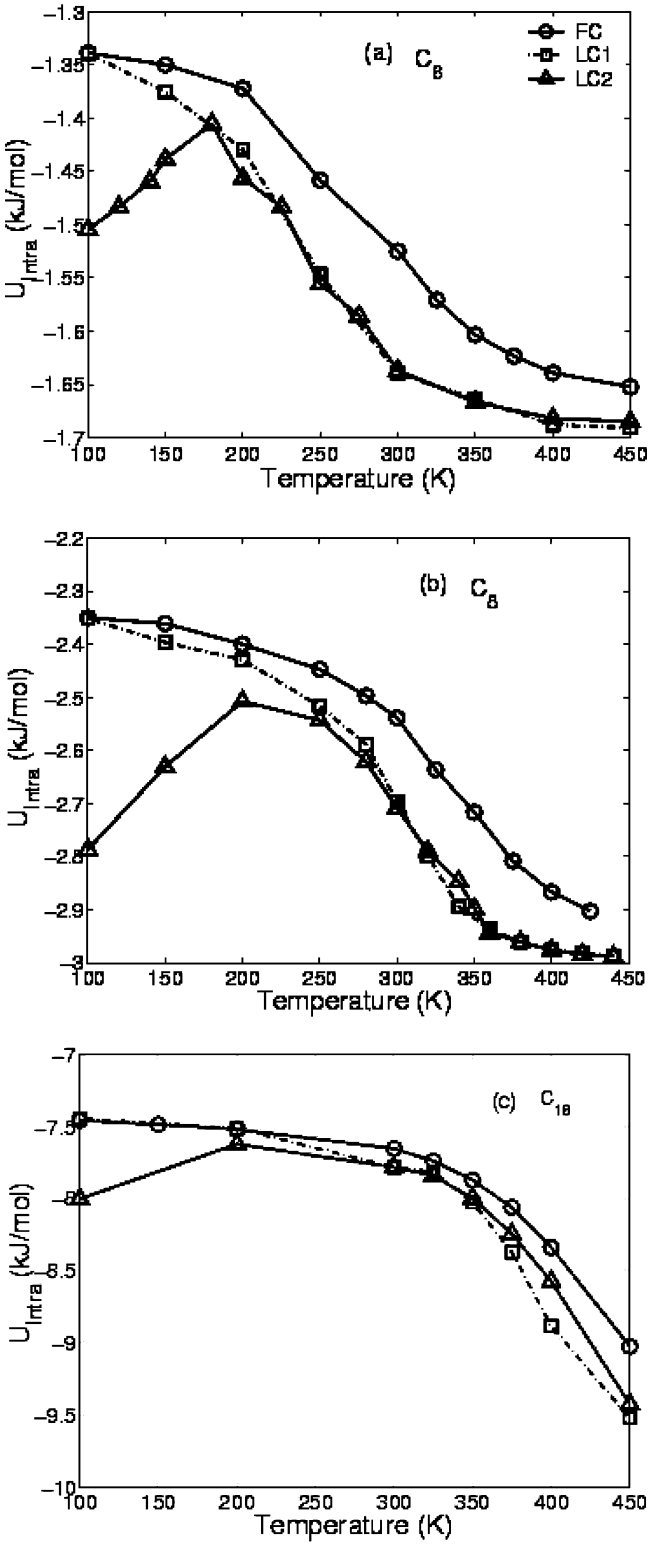

Figure 12. Temperature dependence of the intramolecular potential energy (U_{Intra}) for FC, LC1, and LC2 SAMs for the (a) C_6, (b) C_8, and (c) C_{18} alkanethiols from MD simulation. In contrast to U_T (Figure 11), U_{Intra} for the FC SAMs is always higher than that for the LC SAMs. The temperature at which the U_{Intra} values for the LC1 and LC2 SAMs become identical increases with an increase in chain length.

more than 24 h. As a consequence, the sharp decrease in the integral intensity for C_8 thiol at temperatures (Figure 4a) more than 390 K may be accounted for as primarily due to desorption. It is also important to note that this saturation process does not happen until a high temperature is reached in the case of the longer-chain C_{18} thiol, which is less prone to defect accumulation because of the presence of strong van der Waals forces between chains. The defects continue to accumulate and continue to increase monotonically with temperature until 390 K without showing any signs of arrest for the C_{18} alkanethiol. We contend that this is a basic difference in the thermal

performance of short- and long-chain molecules, and the difference is also borne out qualitatively by the IR peak frequency data, which shows the order/disorder of C_8 thiol molecules in the 320−390 K range (Figure 3) to be more or less insensitive to temperature change while the disorder of the C_{18} thiol molecule continues to increase monotonically until about 400 K. It is of great interest to note that the conclusion that the C_8 thiol, in a situation of thermal change in a practical (tribological) range of temperature, is more stable than the C_{18} thiol is also suggested qualitatively by our cyclic voltammetry study where the SAMs are electrically charged in an electrolytic solution.

Domain Growth and Role of Defects. The MD results offer us considerable insight into the structural differences in the thermal characteristics for FC and partially covered monolayers in the presence of line defects. At low temperatures, 100−300 K, the presence of grain boundaries alone (LC1) leads to a faster accumulation of gauche defect with temperature; this trend continues until about 300, 350, and 450 K for C_6, C_8, and C_{18}, respectively. Further, when a SAM is defective because of the presence of domains and grain boundaries, shorter chains accumulate gauche defects faster with respect to temperature rise than longer chains. Freedom of movement of chains due to LC not only increases the tilt angle but aids in a faster untilting with temperature rise where the chain length is shorter, and by the above argument, the molecules are more defective than in the case of longer chains. When gauche defects are deliberately introduced (LC2) in a partially covered SAM, the defect accumulation in the 250−450 K range is not affected greatly though it appears to reduce untilting for longer-chain molecules.

We observe that the line defects as shown in Figure 1 are asymmetric in the y direction. Simulations with C_6 alkanethiols with an initial configuration having a symmetric (y direction) defect structure yielded similar values for all the system properties evaluated in the temperature range 100−450 K. However, a difference of less than 2° was observed in the system tilt at lower temperature (100−150 K) with the symmetric defect structure having the smaller tilt angles. In this temperature range the differences in the intermolecular potential energies and the substrate potentials between the two defect structures were less than 1 kJ/mol.

To assess system size effects for the LC1 and LC2 SAMs we carried out extensive simulations for C_6 with a simulation box size of $L_x = 178.94$ Å and $L_y = 86.10$ Å. For the FC SAM this corresponds to a system with 720 thiol molecules, and for the LC SAMs the number of molecules was 682 ($\rho_s = 20.27$ Å^2/chain). For the LC SAMs the surface density is 2.32% larger than the smaller system size. Although the trends observed with the larger-system-size LC SAMs were similar to those observed in the smaller system size, tilt angles in the larger system size were lower by about 3° and the gauche defects were reduced by about 1.5%. The differences in the total potential energy of the monolayer were within 1 kJ/mol.

In the case of LC1 SAMs the line defects that are introduced in the initial configuration of the monolayer (Figure 1) were eliminated by about 150 K for C_{18} and 200 K for C_8. These temperatures are likely to be influenced by the pattern of the line defects and its periodicity within the monolayer. However, we did not investigate this issue further. X-ray studies[16] have also shown that it is possible to increase the domain size dramatically at relatively low temperatures (360 K) for SAMs of short-chain alkanethiol ($<C_{14}$) in comparison to what is possible for the long-chain molecules ($>C_{14}$). The longer-chain thiols are generally difficult to anneal and show a steady increase in frequency until heated to temperatures above 400 K. It is clear from Figure 3 that for C_8 molecules at 300 K only a modest amount of thermal energy is needed to bring the molecule to a state where its order becomes insensitive to increases in temperature, in the 300−370 K range. This is in marked contrast to the C_{18} thiol behavior (Figure 3) that shows a steady increase in disorder in this temperature range.

The above discussion, thus, points in the direction that the reduction of van der Waals forces due to shortening of chains allows rapid accumulation of defects in the short chains in response to heating. The defects appear to saturate at a certain critical temperature; the longer the chain length, the higher is this critical temperature. We note that the annealing behavior observed here for the LC2 films is primarily a consequence of the film being away from its equilibrium state. Because all simulations are carried out at thermodynamic equilibrium, the degree of annealing and the temperature range over which it occurs is naturally dependent on the defect population in the starting configuration and the duration of the MD simulation at the lower temperatures. Quenching from a high temperature configuration to lower temperatures serves only to trap defects resulting in a metastable state. We point out that the purpose of these simulations with the LC SAMs is to primarily illustrate the qualitative features of defect annealing.

Conclusions

On the basis of grazing angle infrared spectroscopy of self-assembled short- and long-chain thiols on gold over a 300−440 K temperature range, a range of interest to tribology, we conclude that the insensitivity of short-chain thiols to thermal changes when compared with the long-chain thiols in the 300−390 K temperature range is due to the inherently greater disorder in short-chain thiols at 300 K. The data obtained by cyclic voltammetry on SAMs in electrolytic solution and subjected to an electric field suggest a similar conclusion. Our MD study not only supports this conclusion but is also able to explain the morphological changes associated with the stability characteristics. The short-chain thiols untilt rapidly in the early part of the thermal history. At 360 K the C_8 SAM is saturated with defects and acquires a randomized aggregate morphology, arresting further disorder until a temperature close to 400 K. The longer-chain molecules, on the other hand, collect defects much more slowly principally by the accumulation of gauche defects and continue to disorder monotonically with increasing temperature to a temperature (>400 K) much higher than what is observed for the shorter chains.

Acknowledgment. We thank the support provided by Center for High Technology, Ministry of Petroleum, Government of India. We also thank scientists and engineers from Indian Oil Corp. (R&D) and Indian Institute of Petroleum for valuable discussions. We thank G. Rajesh for his help in electrochemical studies. We would also like to thank Dr. S. Balasubramanian for several useful discussions while implementing MD simulations.

LA048654Z